# Abstract paper on the thesis Basic Structures of Matter

## (Thesis about matter, space and time)

### S. Sarg

**Abstract of the paper**. A model of unified field theory is built by using a more general concept about matter, space and time. The known physical laws and postulates are obtainable if the classical empty space is filled by unique structure of matter. A model called a Cosmic Lattice (CL) is suggested according to which the vacuum possesses a unique grid structure built of two types of super dens sub-elementary particles arranged in nodes. These particles called twisted prisms are from two different intrinsic matter substances. In empty space the prisms of same type are attracted by Intrinsic Gravitational (IG) forces inverse proportional to the cube of the distance. The IG field of the prisms possesses axial anisotropy and rotational component due to a lower level structure. Each node is formed of four prisms of same type, while intrinsic energy balance assures gaps between the alternatively arranged nodes. The flexible geometry of the single CL allows complex oscillations with two kind of periodical cycles, a spatial anisotropy and energy well. So the CL space exhibits quantum features, a distributed zero point energy and provides conditions for fields; gravitational, electrical and magnetic. It is also responsible for the constant light velocity, the relativistic effects and the inertia. The elementary particles are complex helical structures built of twisted prisms in a unique process of crystalization. The protons and neutrons in the atomic nuclei follow a strict order with pattern signature of the Periodic table. The spatial arrangement of the quantum orbits is defined by the nuclear structure. The suggested physical models are successfully applied for explanation of dozens of physical effects and phenomena in a range from elementary particles to cosmological events. The concept of the vacuum structure leads to the conclusion that some of the adopted by the contemporary physics laws and postulates are not absolute.

**Keywords**: *Unified field theories, superstring theories, intrinsic matter, twisted prisms*, *helical structures, atomic nuclear structures, zero point energy, light velocity.*

**Note**: *The equation numbering in the abstract paper corresponds to the numbering used in BSM thesis.*

The study of the Universe requires physical explanation of the natural phenomena in quite broad range of space and time. Many common parameters between the the phenomena of micro and macro cosmos indicate that one single unified field theory is needed. Number of attempts for creation of such theory are made. Instead of one broad range theory now we have a bunch of individual theories. While providing model explanations in own particular range they are often contradictable in the broader range of space and time. Among these theories are: the theories of the particle physics, the Quantum mechanics, the theory of Relativity (General and Special) and the theory of Big Bang. One of the tendencies of the contemporary physics is to extend the individual ranges of the existent theories in order to integrate them into one unified theory. Such approach, however, appears not quite successful. Another alternative way is followed by the superstring theories, but they need multiple space-time dimensions.

One of the problematic aspects of the contemporary physics is the underestimation of the principles of the causality, the real objectivity and the logical understanding. The adoption of such approach is influenced by the successful mathematical models introduced by the quantum mechanics. The Quantum mechanics is undoubtedly a successful theory. At the same time it is so bizarre, from the point of view of human logic, that Richard Feynman, a master of quantum calculation said: "nobody understand the quantum mechanics" (how it works). Albert Einstein in his paper "Can Quantum-mechanical description of physical reality be considered complete?" writes: "Every element of the physical reality must have a counterpart in the physical theory" (Phys. Rev. , 47, 777-780, (1935)).

The mathematical methods today are quite more advanced, but this feature does not exempt them from the necessity to comply the Einstein's comment.

The physical logic in the methods of contemporary physics is significantly obscured. One of the main reasons is the underestimation of the causality principle and its replacement with a probability. In other words the cause is replaced by the chance. This works well for the quantum mechanical models, but it could not be accepted as a rule in the nature. The study of complex systems by a classical way shows that any physical system could be discribed by more than one mathematical models. From this point of view the mathematical model of the quantum mechanics could not be postulated as a unique.

The underestimation of the physical logic could be demonstrated by the fact that number of phenomena now are accepted without any logical explanation. The following questions, for example, have never got satisfactory answers:

- Why the light velocity is a constant?

- What is behind the space curvature around a heavy material object?

- What are the boundary conditions of the wavefunction describing the photon?

- How could the single photon be polarised?

- How could the single photon interfere with itself?

- How could energy exist separated from the matter? (In the case of the initial singularity in the Big Bang and the final singularity in the Black holes)

- If the Universe contains a finite matter and some photons are emitted in empty space, what happens with their

energy?

The last three problems in fact show infringement of the energy conservation principle.

In order to avoid the logical explanation of some of the above questions, postulates have been introduced. The quantum mechanics and the theory of Relativity have accepted large number of postulates in a form of rules. In the modern physics the following opinion is adopted: The equation of the quantum mechanics works by some magical way, but they works (of cause not for everything). An opinion is gradually imposed that a logical physical understanding is not necessary. As a result, many postulates adopted in the beginning of the 20th sentury have note be reexamined seriously in the last 50 years.

In addition to the mentioned theoretical problems, many of real phenomena are not satisfactorily explained. For example: Casimir forces, zero point energy of the vacuum, rules and violation of rules in particle physics, physics of FQHE, electrogravity, levitation in superconductivity, solar neutrino problem, redshift periodicity in observation of distant cosmological objects, the physics of globular clusters, galactic rotational curves and "dark matter", dipole anisotropy of CMB (Cosmic Microwave Background), X-ray background, Lyman alpha forest, Gamma ray bursts, deviation of Hubble velocity-distance relation from linearity at $z > 0.8$ and so on.

In the recent years the imaging technology based on tunnelling microscopy marked significant advances. The obtained spatial resolution is comparable with the interatomic distances in artificially grown crystal layers. Relying on the existing mathematical model of the atom some researchers provided a conclusion that they see the wavefunctions, so the quantum model is a real physical model. Such conclusion, however, it is not true. There is a hardware structure behind the image and this is a necessary condition even from a common logical sense. The quantum mechanics is built on the concept of the Bohr (planetary) atomic model. It may provide good mathematical representation from energetic point of view, but this is not enough to be accepted as a real physical model. (The physical problems of this models are well known: a lack of boundary conditions, a lack of explanation how the complex orbits are supported by the intrinsically small nucleus, and lack of satisfactorily physical explanation of the quantum conditions and the finite lifetime of the exited states).

It could be useful to make a comparison between the basic logical concepts adopted into two different fields: the computer science and the quantum mechanics. In the first one the unbreakable human logic is a basic rule. In the second one the human logic is excluded and replaced by rules.

The BSM theory applies a different approach, relying on the common sense logic and complying to the Einstein's comment from 1935. According to BSM, the nature has its own hard rules and the processes from micro to macro-world are not so probabilistic as admitted in the quantum mechanics. If all the phenomena exist in three-dimensional space and one direction of time they should be understandable by the human logic. In such aspect the initial goal of the BSM analysis was to find out what is behind the postulates and the rules. The adopted postulates should be reduced to a minimum number, containing mailnly those for which we have enough observational confidence. In such aspect the following three basic postulates are defined:

- **The energy conservation principle**
- **The energy could not be separated from the matter**
- **The gravitation is a form of energy exchange between intrinsic matter objects involved in the total energy balance of the system**

The first postulate is quite well verified. The second postulate is in complete agreement with the common logical sense. The third postulate is apriory accepted, but the analysis in Chapter 12 puts some light about the possible mechanism of the gravitation. It could be a result of energy balance conditions in a very low level of matter organisation. In such aspect this phenomenon is often referenced as intrinsic gravitation.

Based on these postulates all the necessary rules should be derivable. Some of them could be named as secondary postulates only for convenience but they should be explainable in some point of the analysis (for example the constant light velocity).

**What is the BSM concept?**

The theoretical introduction to the BSM concept begins in **Chapter 2** titled **Matter, Space and Fields**. BSM relies on theoretically discovered two stable sub-elementary particles in the Universe, involved in the underlying structure of the observable space and the complex structure of the atomic particles. They have a shape of hexagonal prisms with length to diameter ratio > 1. The two types of prisms with dimensional ratio of 2:3 are made of different substances of intrinsic matter. The BSM analysis finds that the prism lengths are in the range of $(1 \sim 10) \times E^{-21}$ (m). Both types of prisms possess similar internal structures with axial twisting in opposite direction. As a result of this feature their intrinsic gravitational field exhibits axial and twisting anysotropy simultaneously (these features becomes more apparent in the latest chapters but more detaled analysis is presented in Chapter 12). The BSM concept uses a model of two type of externally twisted hexagonal prisms with a same geometrical ratio of 2:3. The mathematical models based on externally twisted prisms allows to simulate quite successfully the intrinsic features of the real prisms at higher level of matter organisation up to the atomic particles. In such aspect the lower level structure is temporally ignored in the analysis. The adopted model also have well defined ratio between the volume of the twisted peripheral part and the cen-

tral part, a feature that is successfully used in the analysis of complex interactions. Put in empty space (in a classical sense) a pair of twisted prisms of same substance is attracted by **Intrinsic Gravitational (IG) force, $F_{IG}$, that is inverse proportional to the cube of the distance, r (inverse cubic IG law)**. So the IG atractive force between two axially allignd prism of same type is:

$$F_{IG} = \frac{G_0 m_0^2}{r^3} \qquad [(2.1)]$$

where: $m_0$, is the intrinsic mass of the single prism, $G_0 = G_{0S}$ - is IG constant for prisms of same substance and $G_0 = G_{0D}$ I- is IG constant for prisms of different substance. For condition of not aligned axes a cosine factor could be used.

The relation between the both constants $G_{OS}$ and $G_{OD}$ is discussed in Chapter 12, where a concept of the physical meaning of IG forces and IG energy is developed. For the analysis in Chapter 2 it is only accepted that the algebraic relation $G_{OS} > G_{OD}$ is valid, when referencing to a common length unit. later in Chapter 12 it becomes more apparent that they may have an opposite value in a normal CL space and such relation is controlled by a complex intrinsic energy balance at the very low level of matter organization. At such condition we may have opposing forces

$$F_{IG(1)} = -F_{IG(2)} \qquad (a)$$

where: index 1 and 2 denotes the first and second type matter substance (right and left handed prism)

Note that the balance condition (a) depends of gaps between uniformly mixed spatial lattice from the two type of prisms.

The inverse cubic law for IG is extensively used in number of developed models and expressions about existing phenomena, according to BSM theory. They are cross validated by results from different physical fields.

**One of the main distinguished concept of the BSM theory is that: the vacuum possessses a underlying material structure.**

BSM suggests a model according to which this structure is formed by equally distributed two type of nodes (right and left handed). Each node is formed of four prisms of same type with prism axes at 109.5 deg for geometrical equilibrium. Every node of right-handed prisms has four neigbouring nodes of left-handed prisms and vs versa. **The node stability is kept by the condition [(2.1.a)] while the gaps between the nodes by the condition (a)**. These features of CL structure allows a limited, but well defined freedom of the connected CL nodes to posses a vibrational motion. The analysis of the single node dynamics shows that there are two set of axial simmetry as shown in Fig. 2.20.

The axes a,b,c consides with the prisms axis at geometrical equilibrium, while the axes x,y,z are orthogonal. The axes ,x,y,z of the neigbouring CL nodes coincides. The oscillation conditions of the single CL node are characterised by 3 orthogonal axes, denoted as *xyz* axes and 4 axes along the prism central axes at 109.5 deg, denoted as *abcd* axes.

Every single node in such lattice has one unique feature: **For conditions defined by the inverse cubic IG law in respect to its neigbours the geometrical equilibrium position of the node is not stable.** This is evident from Fig . 2.21 and Fig. 2.23 illustrating the return forces for a node deviation along anyone of axes *abcd* or *xyz*.
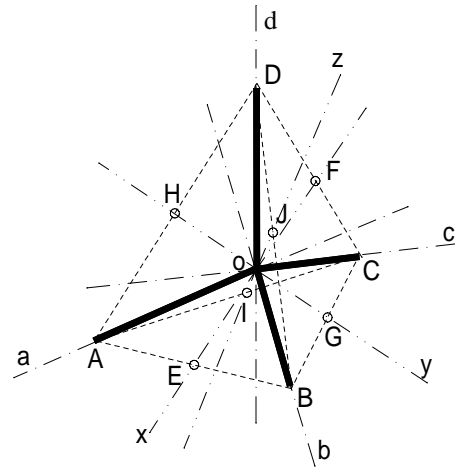


Fig. 2.20
CL node in geometrical equilibrium position
The two set axes of symmetry are: *abcd* and *xyz*

Fig. 2.21 and Fig. 2.23 show that the return forced for node displacement respecively along xyz axes and along abcd axes.
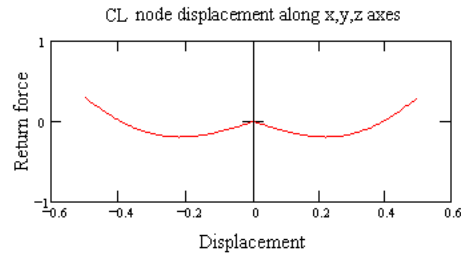


CL node displacement along x,y,z axes
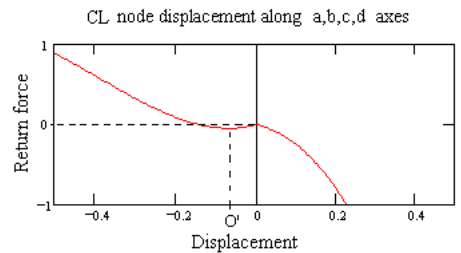
Fig. 2.21



CL node displacement along a,b,c,d axes

Fig. 2.23

Fig. 2.24 shows the node energy diagram of CL node. The condition of return forces along xyz and abcd axes are superimposed. This allows definition of two energy wells denoted with 1 and 2. In the right side of the diagram the positions of some critical energy levels are defined.

Taking into account the IG forces and the dynamical interactions with neighbouring nodes the node trace motion is a multiple loop 3-D curve. In order to describe the energetic properties of a single oscillating node with some space and time characteristics BSM uses two vectors: NRM - Node Resonance Momentum and SPM - Spatial Precession Momentum.
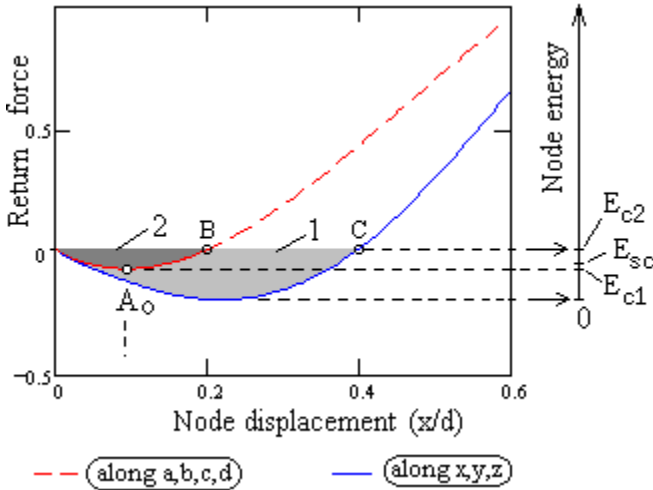
Fig. 2.24 Node energy diagram of oscillating CL node

The NRM cycle defines the node resonance frequency. The trace curve of NRM could be approximated by a plane curve but any selected initial and final points for one full cycle do not coincide, as shown in Fig. 2.26.
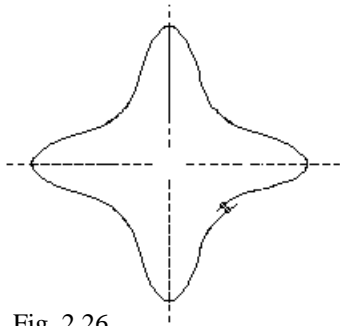


Fig. 2.26

The SPM cycle is obtained when the node trace passes through a same initially selected point. This happens for many NRM cycles. This number denoted as $N_{RQ}$ is calculated in Chapter 2: $N_{RQ} = 0.8843 \times 10^9$ It is found that this parameter is directly related to the permeability of the vacuum The spatial momentum density of SPM vector for one full cycle is presented by 3-dimensional surface denoted as a quasisphere (because it possesses six bumps aligned with *xyz* axes and four dimples aligned with *abcd* axes.) The oscillation properties of CL nodes provide the Zero Point Energy (ZPE) of the CL space. Its measurable parameter is the CL space background temperature of 2.72 K. (known so far as a signature of relict radiation). BMS provides theoretical formula for its calculation. In domain of CL space without electrical field the shape of the SPM quasisphere is symmetrical as shown in Fig, A.a. It is denoted as a Magnetic Quasisphere (MQ). In CL space domain in which electrical field is present the SPM quasisphere is deformed to a shape shown in Fig. A.b. It is denoted as Electrical Quasisphere (EQ). In a free space (without presence of electrical and magnetic field) MQs of the neighbouring nodes are commonly synchronized in domains, denoted in BSM as magnetic protodomains. These protodomains define the accurate value of the vacuum per-

meability. In the same time they are in continuous recombination, an effect denoted as Zero Point Waves. The latter feature is responsible for the uniformity of the ZPE of CL space. The vacuum parameter: permittivity of free space, $\varepsilon_0$, is defined by the average deformation of the CL node quasisphere participating in the wavetrain of the quantum wave with energy of 511 KeV. So $\varepsilon_0$ corresponds to EQ with defined ratio between the shorter and longer radii along xyz axes.
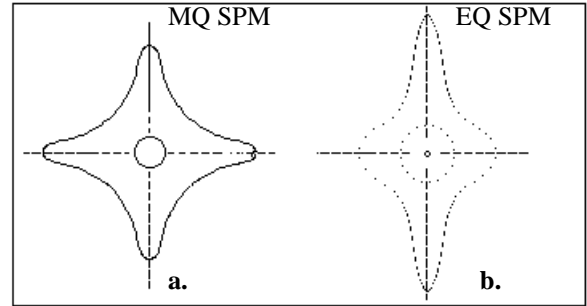


Fig. A

The EQs and MQs define the quantum features of CL space. The energy of EQ, however, is larger than the energy of MQ. EQs may exist stationary only around hardware particle possessing an electrical charge feature. Otherwise, its excess energy (in comparison to MQ) is propagated in a complex wave structure moving with a light velocity. This feature helps to unveil the time-spatial structure of the photon as a complex wavelike structure. The wave structure caries simultaneously the parameters of SPM vector that provides the quantum conditions, so the complex wave is called a quantum wave. The quantum wave involves a large number of EQs and MQs and is analyzed by the method of running quasispheres. The excess energy of every EQ is transferred between two neighbouring CL nodes per one resonance (NRM) cycle. So the light velocity is defined by the average distance between neighbouring node in xyz coordinate system per one resonance (NRM) cycle. The quantum wave (photon) has a complex configuration of running EQs and MQs. While the EQs carry the photon energy, MQs assure the boundary conditions by perfect isolation of the wavetrain in a finite transverse radius. The quantum conditions are defines by the Compton time $t_c = 8.093 \times 10^{-21}$ (sec) that is a parameter of CL space.

One cycle of stationary CL node involved in the quantum wavetrain defines the Compton time $t_c = 8.093 \times 10^{-21}$ sec. The constancy of average resonance cycle (over space and time) is maintained by the quantum conditions created by SPM MQ and EQ, related with the parameters $\varepsilon_0$ and $\mu_0$, so the light velocity is defined by the equation: $c = 1/\sqrt{\varepsilon_0 \mu_0}$. Analysing the quantum wave conditions, the basic CL space parameters are derived. It is shown that the light velocity (c) and the Compton frequency ($\nu_c$) are intrinsic CL space parameters. Then the physical constants:

$\varepsilon_0$, $\mu_0$ and $h$ are completely defined by the CL space parameters.

The CL nodes have one additional important feature. Due to the partial freedom and even spatial distribution some amount of nodes could be separated from the lattice, partly folded and existed in this form inside the CL structure but only in continuous motion. They play a crucial role for the inertial properties of the atomic matter in CL space. This feature makes the CL structure quite unique and distinguishable from any concept of idel gas. In the same time it allows to provide a classical explanation of the concept of the inertial frame according to the Theory of Relativity. Using the known physical constant, BSM, was able to express some of the basic parameters of CL space: the Static pressure ($P_S$), the partial pressure ($P_P$), the Dynamical pressure ($P_D$) and the Compton wavelength. The Compton wavelength, the Plank's constant and the unit electrical charge apear strongly related with the CL structure parameters.

The atomic matter is built of three stable particles: proton, neutron and electron. All of these particles are comprised of complex helical structures, built of prisms. Every helical structure of first order have internal lattice denoted as radial lattice that is much dense that CL and usually twisted. So this lattice is able to modulate the CL node quasisphere making it EQ type. In such case an electrical field is created, but the far field appearance of such particle depends also of its 3-D geometry. The proton and neutron have one and a same compositions of helical structures, so only their overall shape distinguishes them. In neutron the electrical field is locked in proximity by the symmetrical IG field and it appears as a neutral in far field. The proton has different shape than the neutron and the electrical field is unlocked, so it exhibits a charge. The charge of any single helical structure is always unity due to a balance between the intrinsic IG forces and CL space. The subatomic particles are obtained when a stable particle as proton (neutron) is destroyed and they have a finite lifetime. Some particles may partly change their geometry, but the mechanism assuring the unity charge is always valid. The sign of the charge is defined by the chirality of the twisted prisms. Then the two types of prisms are referenced as positive and negative in order to avoid an incorrect assignment of the chirality (but this attribute itself is not equivalent to the charge).

Any helical structure with proper configuration is able to posses a charge. Such kind of charge is inseparable feature of the helical structures and is denoted as a real. The CL space environment, however, provide additional possibility for a charge existence without a helical structure. This charge is a wavelike structure of EQs and MQ arrangement, but having only one type of EQs without boundary conditions of MQs. Such charge could not be stationary. It may propagate only with light velocity, but the charge constancy could not be preserved as in the case of a real charge particle. So such charge may imitate a real charge. BMS refers to such wave as a quasiparticle wave as it imitates a charge particle, but usually possessing a high energy. Such kind of charge is created during the transition state of the structural modifica-

tion of a particle that looses a far field E-field due to the overall change shape. This happens in convention of proton to a neutron. Examples for quasiparticle waves are some beta particles generated in the radioactive decay of the elements. In this case the high energy of the quasiparticle waves is contributed additionally from the IG energy released from the nuclear conversion.

In **Chapter 3** titled **Electron system** the structure and dynamical properties of the oscillating electron are analyzed. The electron is a system of three helical structures one inside another, as shown in Fig.3.2. For this reason it is more often referenced in BSM as an electron system. The external shell is built of negative prisms, the internal one - from positive and the central core - from negative. The external and internal shells also enclose twisted internal structures of same type prisms, called Rectangular Lattice - twisted (RL(T)). Only the most external RL(T) is able to modulate the SPM quasispheres in the surrounding CL space, converting them to EQs with proper spatial configuration. This type of modulation is the electrical charge of the electron, stabilized to unity by the IG forces. During the electron motion the internal structures oscillate in conditions of ideal bearing interacting with the EQ and MQ CL space (electromagnetic type of interaction). In the same time its inertial properties are result of folding and unfolding of CL nodes displaced by the high density (RL(T)) structures with helical core envelope. The electron system (electron) possesses two proper frequencies, one of which is equal to the Compton frequency of the CL space. The motion of such system in CL space is characterized by strong quantum features. It is found that its confined motion exhibits preferred quantum states of its velocity, due to interactions with the oscillating CL nodes. They correspond to the energy levels: 13.6 eV, 3.4 eV, 1.51, 0.85, 0.544, 0.3779. If the internal positive shell with its internal negative core is out of the external negative shell, we may say that the electron system is decayed into degenerated electron and free positron. The free positron also exhibits a quantum motion, but it is a simpler oscillating system possessing only one proper frequency. The proper frequency of the free positron is twice larger than the Compton frequency, but when it is inside the electron it is three times larger. The electron system is successfully used as a probe for derivation of the basic CL space parameters, as mentioned above: $P_S$, $P_D$ and $P_P$ (static, dinamical and partial pressure). **The parameter $P_S$ is involved in the equation of Newtonian mass derived by BSM**. The mass equation of any helical structure is given by the Eq. 3.48:

$$m = \frac{P_S}{c^2}V_H \qquad \text{where: } V_H \text{ is the volume of FOHS} \qquad (3.48)$$

This is the apparent mass of the helical structure matter in CL space, for which Newton's law of gravitation and inertia are valid. Eq. (3.57) given in Appendix 1 is another form of the mass equation. The parameter $P_D$ is related with the zero point waves and ZPE of the CL space. The parameter $P_P$ is related to the inertial properties of the atomic matter (con-

sisting of helical structures in a stable configuration). In Chapter 10 quite interesting result is found: the ratio $P_P/P_S$ appears defined completely by the fine structure constant according to Eq. (10.18).

The relativistic gamma factor is derived from the quantum motion properties of the electron system. When the electron system is activated for strong oscillation it is able to pump CL space and the energy is released as two or three gamma photons. A system of normal electron and free positron, known as positronium is also able to pump the CL space terminating with emission of photons.

The shape and internal structures of the proton and neutron are discussed in Chapter 2 and 6. The intrinsic matter structure of the neutron and proton is one and a same. The difference is only of their overall shape: the neutron is a folded torus, while the proton is a twisted torus whose 2-D projection is given by the Hippoped curve for parameter $a = \sqrt{3}$ (its shape is close to number 8). The shapes of the proton and neutron are illustrated in Fig.6.22 and 6.25 (not in comparative scale). The most external shell of the proton (neutron) is positive. A portion of the internal lattice structure enclosed in the helical structures is illustrated by Fig.2.15.B (not in scale), while Fig. 2.15.A. shows the proton's (neutron's) core section. Inside the envelope formed by the external shell the proton (neutron) contains two pions with opposite charges and one central kaon. The pions are curled toruses containing multiple stretched turns as the single coil of the electron but with much larger second order step. The configuration of the two pions inside the proton amazingly resembles the double helical structure of DNA, but without connecting ladders. They are well centred around the central kaon structure inside the proton (neutron) volume by their proximity fields.

The kaon is a torus in the central axis of the neutron or proton. From outside to inside the internal kaon contains external negative helical shell, internal positive shell and a central negative core. Both shells are helical structures containing internal RL structures. The external positive shell of proton (neutron) and the two internal pions also contain internal RL structures, which are respectively twisted and partly twisted (for pions). The RL structures of the kaon are not twisted. (In such aspect the attributes T - twisted, R- radial are used for RL). The neutron's electrical field is locked by IG forces in proximity to the external shell and does not appear in the far field. This is a result of almost symmetrical appearance of the IG vectors from the internal RL(T) structure of the external envelope. The locked conditions are partly disturbed when the neutron is in motion so it exhibits a magnetic moment. In the proton configuration the geometrical symmetry of the IG field from RL(T), in comparison to the neutron, is disturbed and its electrical field is unlocked. The three compound structures: proton, neutron and electron are stable in CL space.

All types of helical structures normally posses internal RL(T)s, the most external of which modulates the surrounding CL space. Their IG field with defined chirality

converts the symmetrical shaped MQs into asymmetrical EQs (in respect to central point symmetry). An electrical field is created as a result, but only unlocked field could be externally detectable. The lock/unlock conditions are controlled by the IG field of RL internal structures and are dependable of the overall particle shape (for proton and neutron). In the same time the helical structure obtains self adjustable confined shape in CL space, so the unlocked far electrical filed of single structure provides always a unit charge, independently of the matter quantity and the size of the structure. This effect is valid for both - stable and not stable particles as proton, electron system, positron, pions, muons, charged kaons and their temporally existed combinations.

In **Chapter 4**, titled **Superconductive State of the Matter**, the superconductivity phenomena is investigated. The local CL space domain temperature inside a solid body depends of the body temperature. In very low temperature the ZPE of some domains is below the normal level. When ZPE is dropped to some critical level, the SPM vector loses the external synchronization by the zero point waves. In such conditions the SPM vector of the CL node exhibits different behaviour. At some ZPE level, the magnetic and electrical field conditions in the lower energy domains are changed. Then a new carrier is obtained by modification of the electron. The internal positron comes out and attaches to the external negative shell of the electron. This is the main carrier in the Superconductivity State. Such system still has oscillation properties in order to posses a quantum motion but its effective charge appears hidden and the system obtains new unique properties. The diamagnetic effect is a result of a not synchronized repulsive behaviour of the low energy CL nodes. The data of FQHE (fractional quantum Hall experiments) are analyzed and it was found that the changing of the magnetic field in FQHE experiments in fact causes a scanning of the SPM frequency of the low energy domains in a limited range. From the analyzed data it is found that the ratio between the small electron and positron radii is 3:2. But the same proportion must be valid for the prisms lengths. So the ratio 3:2 between the lengths of the two type prisms is found.

In **Chapter 5**, titled **Zero Point Energy of the Vacuum**, a theoretical equation for calculation of the CL space background temperature is derived and compared with experimentally measured one (2.72 K). The participation of the proton (neutron) core length in the derived temperature equation allows a cross validation of the result with the calculations of the proton mass budget in Chapter 6.

In **Chapter 6**, titled **Elementary Particles and their Structures**, the helical structure of the particles with the internal RL structures inside the helical structures are analyzed. Fig. 2.16 illustrate the configuration of the RL structure with not twisted shape and small number of cylindrical layers, for drawing simplicity. The actual number of layers for the positive RL structures is about 20. The parameters of RL structures are unveiled by using some experi-

mental data from the field of particle physics (the estimated masses of Bosons, the tau mass (but used as energies), and the Regge resonance energy at 1.44 MeV). Other used parameters that are experimentally obtained are the "Effective mixing parameter" $\sin^2\theta_{eff}^{lept}$ and Fermi coupling constant. $G_F$ They are essential parameters in the Electroweak theory. The Boson's masses according to BSM are signatures of the stored intrinsic energy of RL structures released in the process of helical structure disintegration. The prisms quantity contained in the internal RL structures of the first order helical structure is much larger that prisms involved in the boundary envelope. So for calculation of the stored IG energy only the volume filled with RL structure could be considered. The analysis of cut kaon and its modifications indicates that during its lifetime it possesses a jet formed of continuously destructed RL structures. Consequently its mass (and the mass of any optional modification of kaon) is overestimated (about 11 times for $K_0{}^L$). This is in agreement with the analysis of the pulsars in Chapter 12 (the pulsars according to BSM are "burning" huge bunches of straight kaon structures obtained previously in the star central region from destruction of protons and neutrons). The interaction between the CL space and the jet of disintegrating RL structures determines their lifetime (and the lifetimes of their spatial modifications). The RL disintegration plays a role also in the lifetime of the muon but it is a second order modified helical structure and the jet appears as tangential so it could reach a light velocity (like the electron) while its axial velocity is low. The kaon is a first order helical structure and the jet is align to its axis.

The internal structure of proton is determined by using the derived mass equation in Chapter 3 and some accurately measured parameters from the field of particle physics. The overall shape of the proton is inferred to be quite close to the Hippoped curve at parameter $a = \sqrt{3}$. The only difference is that the Hippoped curve is a plane curve, while the proton overall shape does not coincide with a plane, but the approximation is pretty close because the ratio between its core length and its thickness is 207.5. The internal helical structures of the proton (neutron) are shown in Fig. 2.15.A and 2.15.B. **The decay $\pi^+ \rightarrow \mu^+ \rightarrow e^+$ is illustrated in Fig. B. The internal RL structure in pion is twisted insignificantly while in muon and electron (or positron) the twisting is completed. The RL twisting causes small shrunk of FOHS volume, but this volume change is proportional to the mass change, according to the mass Eq. (3.48).**

All geometrical parameters of electron system, proton and neutron, internal pions and kaon are estimated by cross calculations using experimental data of different interactions they are involved. Their geometrical parameters are shown in Table 3. and in the Atlas of the Atomic Nuclear Structures.

In **Chapter 7,** titled **Hydrogen Atom,** the physical model of Hydrogen is analyzed. Definition of quantum orbit is also provided with analysis of its attributes and features. Its normal shape defined by the proton's proximity E-field is initially accepted (and proved later in Chapter 9) to be described by a Hippoped curve as the shape of the proton. Based on derived rules and spatial configuration of the quantum orbits the possible orbital planes (called quasiplanes, because they are curved surfaces) of the Hydrogen series are identified: Lyman, Balmer, Pashen, Bracket. A concept of Bohr surface is introduced. It is a closed surface whose spatial position is defined by the orbital plane, while its dimensions are defined by the condition of the orbit with a length of $2\pi a_o = \lambda_c/\alpha = c/\alpha\nu_c$, that appears a limit orbit to the BSM concept. In such case the largest quantum orbit is spatially limited and all orbits of the neutral Hydrogen are inside the Bohr surface. The proton electrical field inside this surface is distributed, but dynamically locked due to the orbiting electron. In such way the the orbits are strictly defined by the protons spatial configuration and the possible quantum orbit. The above shown equation indicates that the length of most external orbit is completely defined by the CL space parameters. The near E-field of the proton only folds the curve with such length in a closed 3-D curve with a proper shape. The quantum space inside the Bohr surface is quasishrunk, i. e. the CL space parameter SPM wavelength (equal to the Compton wavelength) is shrunk - $\lambda_c{}^*$. This is possible if accepting that SPM frequency of EQ nodes is deviated in respect to MQ node frequency. The orbit is quantum stable if its trace length contains a whole number of $\lambda_c{}^*$ wavelengths, as illustrated by Fig. 7.7. A model of Balmer series for Hydrogen atom is built and the calculated energy levels are compared with the observed spectral lines. The Hydrogen model of BSM is completely different than the Bohr model, but possessing the same quantum levels. The accurate mathematical model when using the BSM concept could be quite complex, but the simplified BSM Balmer model provides enough confidence about the real physical configuration. One important feature of the BSM Balmer model is the boundary limit of the possible electron orbits.

In **Chapter 8**, titled **Atomic Nuclear Structures**, the rules of atomic nuclear configurations for all elements from Hydrogen to the upper stable elements are unveiled. They are strongly consistent with: the pattern of the Periodic table (rows, columns, groups, valence); the Hund's rules; the Pauli exclusion principle; the oxidation number of elements; the first ionisation potential; the X-ray properties of the elements; the spin-orbital interactions. The quantum number and the position of the electron orbits are defined by the nuclear configuration. Additionally presented or discussed topics are: X-rays properties of the atoms, spin-orbit interactions, nuclear magnetic resonance, giant resonance, photon emission and absorption, polarized resonance scattering. The BSM model of the atomic nuclei and the electronic orbits differs significantly from the existing so far models, where the electron is considered as a structureless particle and the

proton and neutron are very small pointlike structures. The main discrepancy comes from the interpretation of the scattering experiments. When the CL space parameters and the complex particle structures are not involved in the scattering model, the obtained results differ tremendously (by few orders of magnitude). BSM revises qualitatively the results of the scattering experiments pointing out the missing interactions in the models. In the end of Chapter 8 a feromagnetic hypothesis is defined. Its goal is to explain the three specific properties of the atomic matter in CL space: feromagnetism, paramegnetism and diamagnetism. Fig. 8.23 and 8.24 show a mock-up model of atomic nuclear structure.

In **Chapter 9**, titled **Molecules**, the connections of atoms in chemical compounds are discussed. The atoms in molecules emitting band spectra are connected by quantum orbits that have been defined in Chapter 7. Fig. 9.3 shows in a common scale the projected 2D shapes of the basic atomic structures (nucleus): proton, neutron, deuteron, helium and the possible quantum orbits. The complex vibrational-rotational motion of atomic nuclei in diatomic homonuclear molecules has been analyzed by a classical approach, but using some new discovered features as: quantum orbit conditions, a quantum quasishrunk space in ordered electrical field around the orbital trace, and IG interactions between two nuclei in proximity. A new product, referenced as $C_{IG}$ factor is discovered and estimated as $C_{IG} = G_0 m_{p0}^2$, where $G_0$ - is the IG constant in CL space, $m_{p0}$ - is the proton (neutron) intrinsic mass. It is found that the emitted photon energy appears as energy excess in the IG energy balance between the involved atomic nuclei. A model of such energy balance between diatomic molecules is derived. Based on this model vibrational levels for some transitions of $H_2$ ortho-I and $D_2$ are calculated. The results show a remarkable coincidence with the measured optical and photoelectron spectra. The simple configuration of $H_2$ ortho-I is shown in Fig. 9.12. The calculated energies of the vibrational levels and their comparison to the levels obtained by spectroscopic data are illustrated by Fig. 9.24. The fractional difference between the levels calculated by BSM model and the observed levels is within ±0.35 %.

The proposed model of BSM provides physical explanation of the vibrational-rotational spectra of the molecules. Its usefulness is also demonstrated by identification of the different configurations of $O_2$ molecule, including those providing "forbidden" transitions in the laboratory conditions but observed in the upper atmosphere. The developed concept is less accurate for heteronuclear diatomic molecules, but it still allows determination of their spatial configuration and bond orientations. In such aspects it is in good agreement with the VSEPR model for molecules. Based on the BSM concept the possible configurations of number of molecules are shown in Chapter 9. In this paper possible states of some selected molecules are shown: $H_2$ - ortho-I (Fig. 9.12); different states of O2 (Figures: 9.43, 9.44, 9.45); ozone $O_3$ (Fig.

9.53.A); $OH^+$ (Fig. 9.54); $CO_2$ (Fig. 9.56); $H_2O$ (Fig. 9.59); $Cl_2$ (Fig. 9.7).

The factor $C_{IG}$ derived by the vibrational oscillations of $H_2$ has been verified by approximative method for calculation of disintegration energy of Deuteron into a proton and neutron. The calculated value differs only by 3.4% from the known binding energy.

In **Chapter 10** titled **Time, Inertia and Gravitation in CL space** the inertial properties of the matter in CL space are analyzed. In CL space environment the inverse cubic IG law from the elementary particles is leaking in very small distances providing some kind of proximity fields. In large distances only the Newton's inverse square law is valid for gravitational interactions between objects of atomic matter. The inverse cubic IG law, however, determines the boundary CL space conditions between two massive objects with external CL spaces. Every astronomical object with a large mass as a star, planet, satellite or large asteroid possesses own CL space , permanently connected to the object end extended beyond its solid surface. The boundary conditions between the CL spaces define a separation surface (SS) around every massive object.

If a massive object with its own local space is moving in the local space of a more massive object its SS shape is modified. For a planet rounding a star the SS has a shape of egg that may approach a sphere if the ratio of the star to planetary mass is large. The CL nodes from the external space are folded when passing through. This effect provides a physical explanation of inertial frame used in the theory of Relativity. Inside the SS the local CL space provides local conditions for the light velocity.

The helical structures may also have own CL space in proximity to the external shell. A small body above some minimal mass may oslo have some internal local CL space, around the helical structures of heavier or closer atomic nuclei. Investigating the motion of the electron in CL space it was able to define the parameter Partial CL pressure, as CL space attribute related with the energy momentum carried by the CL folded nodes. Its ratio to the Static CL pressure (defined in Chapter 3) appears to be a function only of the fine structure constant.

$$P_P/P_S = \alpha^2/\sqrt{1-\alpha^2} \qquad [(10.18)]$$

The analysis allowed also to define one useful parameter called **inertial force moment** ($E_{IFM}$).

$$E_{IFM} = h v_c \frac{v}{c} \alpha \quad [Nm] \equiv [J], \text{ where: v - is the motion}$$

velocity, h - is the Plank's constant, $v_c$ - is the Compton's frequency, c - is the light velocity, $\alpha$ - is the fine structure constant.

The parameter $E_{IFM}$ provides a possibility to explain the First and Second Newton's law about the inertial motion. The parameter $E_{IFM}$ appears to be valid from elementary particles through the atomic matter up to large astronomical object: asteroid, planet, star. For inertial investigation of

astronomical objects the planetary motion is analyzed by using the energy ratio:

$$k_E = \frac{U_G}{\Delta E_{IMF}} \qquad [(8.42)]$$

where: $U_G$ - is a gravitational potential of unit mass at some level above the surface of the planet, $\Delta E_{IMF}$ - is the inertial force moment for the same mass

For $k_E = 1$, the Eq. [98.42)] leads to the expression:

$$R_{CR} = \alpha c = 2.18769{\times}10^6 \ (m) \qquad [(10.39.b)]$$

where: $R_{CR}$ is a theoretical critical radius of a astronomical massive body with a circular shape, extended CL space and away of any external gravitational field (free CL space).

Plotting the $k_E$ parameter versus the  mean volumetric radius for the planets shows an excellent alignment of their position on a line, defined by Eq. [(8.42)]. Some small deviation of the position trend, however, is clearly apparent near the value of $k_E \approx 1$, that corresponds to the theoretical radius $R_{CR}$. The analysis of this phenomenon leads to a concept that for planets with mass above some critical value (depending also from the distance from the star and the orbital eccentricity) the atomic matter in the central part of the planet is crushed into bunch of kaon-like structures. This structure is kept, however, stable due to the surrounding domains of dense atomic matter. In such conditions a kaon type of nucleus is formed. The basic feature of such nucleus is that it creates **conditions for super strong magnetic field.** So it should be valid not only for the planetary but for the star magnetic field as well. A **magnetic field hypothesis** for astronomical size object is proposed. This concept obtains strong additional confirmations in the pulsar phenomena, and the processes of dying star, analyzed in Chapter 12 (Cosmology). The analysis leads also to the conclusion that the magnetic field of the star is related to the inertial interaction with the home galaxy CL space, facilitating the folding/unfolding process of  CL nodes in the separation surface zone. In such aspect a peeling mechanism hypothesis is proposed. The latter is in agreement to the concept of feromagnetic hypothesis, defined in Chapter 8.

Chapter 10 provides also analysis about: balance of intrinsic energy for moving body in CL space; reactive energy in the SS between two CL spaces; close distance limit (in the microscale) of the Newton's gravitational low; a possible explanation of the observed gravity waves phenomena in the Earth atmosphere; explanation of the relativistic effects ; considerations for a long space travel.

**Chapter 11** titled **Relation between BSM theory and the modern physics** provides discussion about the relation with the classical theories as: the Newton's mechanics, the Quantum mechanics, the Theory of Relativity and some aspects of the particle physics. The models of the BSM theory work quite well in different fields of physics without contradictions.

In **Chapter 12,** titled **Cosmology**, the cosmological aspect of the BSM as a unified theory is discussed.

About 25 weak points of the Big Bang theory are identified: 5 - from theoretical and 19 - from observational aspect. The BSM analysis leads to a quite different concept about the Universe and the galaxy formations:

- The intrinsic matter never disappears
- The Universe is a stationary
- The intrinsic matter of every galaxy undergoes through a cosmological cycle involving three main phases: prisms recycling, particle incubation (crystallization), and a galaxy active life. The first two phases are hidden.
- The intrinsic matter quantity contained in any prism from different galaxies is a constant due to a specific effect of a matter energy balance with a large hysteresis. This feature is denoted as a **quantum dose mechanism.** Conditions for this mechanism may exist in one of the hidden subphases of the galaxy recycling.
- The atomic level matter of every galaxy operates optimally in own CL space. Put in foreign CL space this matter becomes much colder
- CL spaces of different galaxies are not mixable, so they are separated by Galaxy Separation Surfaces (GSS). This non-mixability comes from the slight difference in the diameter to length ratio of the prisms from different formations. It is a result of difference in the molding forces. The molding forces are dependent of the total matter quantity of the individual galaxy. The latter parameter is different for the different galaxies. A unique quantum dose mechanism, however, assures exactly the same matter quantity in the prisms of same type but from different molds. GSS are quite different than SS, discussed in Chapter 10, and posses different properties.
- The observed large red shift is not of Doppler, but of cosmological origin. The photon (quantum wave) exhibits a small energy loss when crossing the GSS. It is caused by wavetrain refurbishing. The effect of multiple GSS crossing is additive.

In Chapter 12 an attempt is made to infer the lowest level structures of the prisms. To plunge into this difficult task, number of features unveiled in the previous chapters has been used:
- the inverse cubic IG law
- the anisotropy of the twisted prisms
- the twisted prisms are models of basic particles with internal twisted structure
- the fine structure constant shows appearance in different level of matter organization, so it might be embedded in the lowest level structures as a geometrical parameter
- the observable Universe is of matter and not antimatter (this means that the memory of prism's chirality is preserved during the phase of prisms recycling)
- some characteristic frequencies  (the inverse value of Plank's time, the CL node resonance frequency and the Compton frequency) plotted against the level of matter organization show well defined correlation.

In Chapter 12, a concept of **low level structures** as intrinsic matter formations is developed and the conditions

of their growing from bulk intrinsic matter are analyzed. Some postulates had to be initially defined in order to explain the possible growing process. Their logical explanation however becomes apparent in the provided later analysis. Two of the initially defined postulates are:

**P3 A finite quantity of matter is able to handle a finite amount of internal vibrational energy**

**P4 The Intrinsic Gravitation (IG) is a process of external interaction between the formations of intrinsic matter. It involves energy that is a complementary to the total internal vibrational energy of the interacting formations. IG attraction between spatially separated formations is a manifestation of IG interactions.**

The postulate P3 leads to a conclusion that the intrinsic matter quantity may posses a saturation energy level for a defined low level formation.

A concept of intrinsic gravitation as a physical interaction at some super high frequency is developed. For this reason a similarity with the NRM and SPM vector in CL space is used but in different environments. The interaction frequency is attributed to the second point of the level of the matter organization, corresponding to the prism structure. The trend of the level of matter organization is defined by known three points of frequencies: The inverse Plank's time, the node resonance frequency and the Compton's frequency.

The analysis of the low-level structures (below the prism's level) in Chapter 12, indicates that $\alpha$ is a signature of the possible lowest level structure called a **Primary Tetrahedron made of Primary Balls**. The primary balls of two type are accepted as the lowest level intrinsic matter particles with bell shape matter density. So they have a freedom to vibrate in the Primary tetrahedron with common mode oscillations. The signature of fine structure constant propagates in all upper levels of the matter organization. In the lower levels (up to the prisms) the signature of $\alpha$ is propagated from lower to higher order structures. In the higher level of matter organization (the atomic matter) its signature appears in the more complex interactions between the helical structures and CL space. It is embedded in the single coil structure of the electron and the parameters of its confined motion in CL space. It is embedded also into the length of the quantum orbits as a condition for phase repetition of the complex quantum motion of the electron (see Eq. (3.43.i) in Appendix 1). In the analysis of inertia in Chapter 10 the signature of $\alpha$ appears even in the inertial interactions between the astronomical object and the galactic CL space.

A concept of low level growing processes is proposed containing number of phases and mechanisms, but all they are explainable by a classical way. The possible phases are:

- Spherical shaped bulk matter of two substances with total energy above some saturation level

- Formation of alternative (from the two matter substances) homogeneous (by low level structure type) layers at the surface of the spherical bulk nucleus. Anyone of these layers is formed of Quasiball (QB) structures of same congregational order. The layers are not mixable due to the dif-

ference in the IG characteristic frequencies of interactions and the basic dimensional ratio 2:3. Quantum dose mechanism assures the same number of lower level structures in one QB structure.

- Consecutive eruption of the two upper most layers and formation of two spherical clouds

- Conversion of the two spherical clouds into compacifying shells due to IG forces between the matter in the shell

- Crushing of few orders of QBs and molding of prisms formed of lower order Quasi Pentagons (QPs). The QP is a lower level structure comprised of 5 tetrahedrons. with small gaps between them. Then the molded prisms are comprised of stacked QPs with axial alignments. The gaps of the QPs in such stack allow the prism to get a stable twisting - right or left handed. The direction of twisting is predefined by the chiral memory preserved in the existing lower level QBs.

- Galaxy egg formed by two concentric shells in which all prisms of the galaxy matter are included

- Beginning of internal layer pealing mechanism as a double tornado effect. The prisms are released from the molding shells but the pealing effect terminates before breaking the two (internal and external) galaxy eggshells.

- Formation of two cubic lattice structures of prisms of same type inside the galaxy egg (with nodes of 6 prisms). If the right to left handed prisms dimensions are 3:2, the cubic lattice structures of right handed prisms is inside the lattice of lefthanded prisms.

- Phase of helical structures crystallization (the trapping effect mechanism discussed in Chapters 2 and 6 is largely involved)

- Completed crystallization process - formation of of clusters

- Conversion of clusters into torus shaped protoneutrons. In this process the IG anisotropy of the prisms is involved. The new structures are temporally hold by only one straight central helical structure (the latter is similar as the cut kaon).

- Break-up of the protoneutron clusters and releasing of free protoneutrons and formation of electrons from the central helical structures and other broken structures

- Building of CL space domain. They automatically create conditions for electrical and magnetic field. Conversion of the protoneutrons into protons and transfer of IG energy into repulsive E-field energy between the closed spaced protons.

- Break of the external shell of the galaxy egg: beginning of the galaxy birth

- Fast conversion of the free prisms into expanding CL structure. The external layer of this structure may be in initial phase of touching CL nodes (TCL). This phase is propagated as a spherical spatial wave through the empty space until reaching the neighbouring space boundaries. The gravitation inside the TCL formation is propagated with a super light velocity.

- The wave of TCL reaches the neighbouring galaxy CL spaces and interconnections occur.

- Conversion of TCL into CL space. Creation of the necessary CL partial pressure by conversion of normal to folded CL nodes. After the CL space interconnections with the neighbouring galaxies the necessary quantity of folded nodes is equalized by migrated nodes from neighbouring galaxies through GSS.

Despite the large number of processes they may develop quite fast because their time base is much closer to the Plank's frequency (1.855E43 Hz) than to the Compton frequency (1.236E20 Hz).

The described above processes are from the two main phases of the galaxy cycle: phase of recycling and phase of particle incubation. During these hidden phases we could not get any information, because the galaxy egg is separated by empty space. However some phenomena could be observed immediately before the galaxy death or after the galaxy birth. The observed phenomena of the Gamma Ray Bursts, perhaps are signatures of the two possible effects, related with disconnection and reconnection of galaxies CL spaces. The only "witnesses" of the hidden phases of the galaxy cycle are the Globular Clusters (GCs). GC is a cosmological structure of very closed spaced stars with particular behaviour. According to BSM, they are remnants of previous galaxy life that have been able to escape the galaxy collapse. They, perhaps, have been open clusters of stars, escaped from the galaxy collapse but with lost folded nodes (partial CL pressure). Left completely separated with almost zero partial pressure of their CL spaces, they have undergo a fast evolutional process until restoring approximately the ratio between the Static and Partial CL pressure (Eq. 10.18) getting stabilized into formation of globular clusters. These GCs, however, may play important role during the phase of recycling and matter incubation. Surrounding the galaxy egg they may keep it from drifting into neighbouring galaxies. The concept and role of GCs is supported from the analysis of large observational data.

Chapter 12 provides also analysis of additional phenomena like:

- Galaxy nucleus, stored energy and processes around it.

- Factors determining the time duration of the active galaxy life

- Galaxy rotational curves

- Mechanism of pulsations in the Cepheids and emitting layers

- Why the period - luminosity relations between I-st and II-nd type Cepheids are different?

- What happens in the phase of instability of main sequence of the stars?

- The process of star dying and birth of pulsar

- Physics of pulsars as bunch of kaon nucleus with activated jet (single and double jet pulsars)

- What kind is the Cygnus X-1 pair object of supergiant star HDE226868 and X-ray companion claimed as a "black whole"?

- Emitting filaments in Crab nebula

- Continuous X ray background

- Physics of Gamma ray Bursts

- Quasar phenomenon

- What is behind the observed redshift periodicity?

- Lyman alpha forest

- Proposed method for distance estimations in the Stationary Universe

- Non linearity of the Hubble "velocity-distance relation" according to BSM concept (see Eq. (12.50)). Analytical explanation of observed deviation from linearity by the data from high red shift Supernovas (with z - up to 0.8)

- Optical inhomogenity of the Universe and effect of supergalactic clustering

- Negative lensing effect from CL space with large prism's parameter deviation.

## Comments from the author of BSM thesis.

The developed concept of BSM provides a different view about the Universe as conglomerate of recycling galaxies with cosmological time periods. Despite the complex mechanisms and processes the physical unity in a vast scale of space and time is preserved. The energy appears inseparable attribute of the matter and its conservation is valid for all levels of matter organization.

The phenomena related with General and Special relativity are discussed and explained in different places of the theory. The explanation is significantly facilitated when the relativistic effects are analyzed in imaginary absolute frame in which the CL node distance is not uniform, but modulated by the gravitational objects. The unchangeable length of the prism could serve as an absolute etalon for distance. The proton length however is more convenient secondary etalon. For absolute time base the first proper frequency of the electron in free space (Compton frequency) could be used. Using this approach the General relativity effects could be theoretically analyzed without using the complicated Riman's geometry.

All of the provided concepts are supported by observational data. In many cases the physical interpretations from the point of view of BSM is quite different from what has been considered so far but the physical logic and understanding are always present.

Number of details, mechanisms and phenomena discussed in BSM are not mentioned in this paper.

The reader of BSM is advised to follow the consecutive orders of Chapters, because a number of new terms and features had to be introduced. They are initially explained in details, but afterwards they are only referenced by name. Only the first Chapter "Introduction" could be skipped, if the reader has been preliminary acquainted with the Abstract paper of BSM.

The approach applied by BSM appeared to be quite effective and productive. This is a result of the powerful guiding role of the physical logic in the search of the objec-

tive reality. It allows complete orientation in the process of investigation and effective seeding of the needed observational material from the ocean of the experimental data.

The current presentation of BSM could not be considered as a completed or as a final truth. It touches phenomena from different fields of the physics. Any reasonable amendments or critics are welcome. Some technical mistakes are not excluded in the first edition.

# Appendix 1

## 1. Derived equations:

**Notes**: 1. *The equation numbering is the same as in BSM. The first digit shows the Chapter's number.*

*2. Equations (3.13.a), (3.21.a) and (3.42.F), known from the modern physics, are also derivable from the theoretical models of BSM.*

$$R_c = \frac{c}{2\pi v_c} \tag{3.13.a}$$

$$s_e = \frac{\alpha c}{v_c\sqrt{1-\alpha^2}} \quad \text{Helical step} \tag{3.13.b}$$

$$r_e = s_e/g_e \qquad \text{small electron radius} \tag{3.13.c}$$

$$r_p = \frac{2}{3}r_e \qquad \text{small positron radius} \tag{3.13}$$

$$c = \frac{v_R d_{nb}}{k_{hb}} \quad [m/s] \quad \text{light velocity} \tag{2.75}$$

$$\text{where: } k_{hb} = \sqrt{1+4\pi^2(0.6164^2)} = 4 \tag{2.20.a}$$

$$\mu_o = \frac{4\pi m_{CL}k_{rd}^2 c v_c^3}{N_{RQ}} \quad \left[\frac{N}{A^2}\right] \tag{2.52}$$

$$\varepsilon_o = \frac{N_{RQ}}{4\pi m_{CL}v_c^3 c^3 k_{rd}^2} \quad \left[\frac{C^2}{Nm^2}\right] \tag{2.53}$$

$$h = \frac{\pi(c)c^2 m_{CL}N_{RQ}^3 k_d}{4v_c k_{hb}^3} \quad [N\,m\,s] \tag{2.58}$$
$$\text{where: } k_d = \frac{\tau_{511KeV}}{\tau_{CL}}$$

$$q = \frac{N_{RQ}^2}{2v_c^2}\sqrt{\frac{c\alpha k_d}{2k_{rd}^2 k_{hb}^3}} \quad [C] \tag{2.58.a}$$

$$P_S = \frac{g_e^2 h v_c^4(1-\alpha^2)}{\pi\alpha^2 c^3} \quad \left[\frac{N}{m^2}\right] \tag{3.53}$$

$$\rho_e = \frac{m_e}{V_e} = \frac{g_e^2 h v_c^4(1-\alpha^2)}{\pi\alpha^2 c^5} \quad \left[\frac{kg}{m^3}\right] \tag{3.55}$$

$$P_D = \frac{g_e h v_c^3\sqrt{1-\alpha^2}}{2\pi\alpha c^3} \quad \left[\frac{N}{m^2}\right] \tag{3.62}$$

$$m = \frac{P_S}{c^2}V_H \quad [kg] \quad \text{- mass equation of FOHS} \tag{3.48}$$

$$m = \frac{h v_c}{c^2}K_V \quad [kg] \quad \text{- mass equation of FOHS} \tag{3.58}$$

$$\sigma = \frac{v_c\alpha 2}{2c} = 1.09737315\times10^7 \quad [(m^{-1}] \tag{3.21.a}$$

$$\gamma = (1-V^2/c^2)^{-1/2} \tag{3.42.F}$$

$$T = \frac{N_A^2 h v_c(R_c+r_p)^3 L_{pc}^2}{S_w} \frac{1}{2cR_c r_e R_{ig}}\left(\frac{\mu_e}{\mu_n}\right) \quad [K] \tag{5.6}$$

$$T = \frac{N_A^2 hc^2\left(3g_e\sqrt{1-\alpha^2}+4\pi\alpha\right)^3}{864\alpha^3 v_c^2\pi^2 g_e^2(1-\alpha^2)R_{ig}}\frac{\mu_e}{\mu_n} \quad [K] \tag{5.12}$$

$$E_{ZPE} = \frac{1}{2}m_{in}r_{abcd}^2(4\pi^2 v_R^2) \quad [J/node] \tag{5.13}$$

$$r^2 = b^2(1-a^2(\sin(\theta))^2) \tag{6.54}$$

$$L_{pc} = \left[\left(\frac{\mu_e}{\mu_\mu}\right)^2(4\pi^2 R_c^2+s_e^2)-4n^2\pi^2 R_\pi^2\right]^{1/2} \tag{6.61}$$

$$E = \frac{2q}{4\pi\varepsilon_0[L_q(1)+0.6455L_p)]} = 16.01 \text{ eV} \text{ for } H_2 \text{ ortho} \tag{9.4}$$

$$C_{IG} = (2h v_c + h v_c\alpha^2)(L_q(1)+0.6455)L_p) \tag{9.17}$$

where: $C_{IG} = G_0 m_{n0}^2$

$$E_V = \frac{C_{IG}}{q[[[L_q(1)](1-\alpha^4\pi\Delta^2)]+0.6455L_p]^2} - \frac{2E_q}{q} - \frac{2E_K}{q} \tag{9.23}$$

$$\Delta r = L_q(1)\alpha^4\pi\Delta^2 \quad [m] \tag{9.26}$$

$$\Delta E(p,n,\Delta) = \frac{2\alpha C_{IG}(A-p)^2}{[r_n\pm[\Delta r(n,\Delta)]]^2} - pB_{D2}(n,\Delta) \tag{9.55}$$

$$P_P/P_S = \alpha^2/\sqrt{1-\alpha^2} \tag{10.18}$$

$$p_p = \alpha c\rho_e = \frac{g_e^2 h v_c^4(1-\alpha^2)}{\pi\alpha c^4} = 2.19\times10^{-25} \quad \left[\frac{N\,sec}{m^3}\right] \tag{10.22}$$

$$E_{IFM} = P_P V_e = h v_c\frac{v}{c}\alpha \quad [Nm]\equiv[J] \tag{10.11}$$

$$E_{IFM}^G = E_{IFM}\frac{\sqrt{U_{Gn}}}{2\alpha c} \quad [J] \tag{10.59}$$

$$r = \tilde{L}\frac{\ln(z+1)}{\ln(\tilde{n})} \qquad \text{[m]} \qquad (12.50)$$

$$\tilde{n} = \exp\left(\frac{1}{(dN/dz)(z+1)}\right) \qquad (12.52)$$

## 2. Notations:

**Derived equations**                **Table 1**

=============================================

| Eq. No | Parameter | Name |
|--------|-----------|------|
| (3.13.a) | $R_c$ | Compton radius of electron |
| (3.13.b) | $s_e$ | helical step of the electron |
| (3.13.c) | $r_e$ | small electron's radius |
| (3.13) | $r_p$ | small positron's radius |
| (2.75) | $c$ | light velocity by resonance CL node param |
| (2.52) | $\mu_o$ | permeability of free space |
| (2.53) | $\varepsilon_o$ | permittivity of free space |
| (2.58) | $h$ | Planck's constant by CL space parameters |
| (2.58.a) | $q$ | unit charge by CL space parameters |
| (3.48) | m | (Newtonian) mass of FOHS expressed by its volume $V_H$ |
| (3.53) | $P_S$ | Static CL pressure |
| (3.55) | $\rho_e$ | Intrinsic electron density estimated by the Newtonian mass |
| (3.58) | m | mass of FOHS expressed by volume ratio $K_V$ normalized to the electron envelope volume |
| (3.62) | $P_D$ | Dynamical CL pressure |
| (3.57) | $m$ | Newtonian mass of helical structure particle |
| (3.21.a) | $\sigma$ | Rydberg constant by CL space parameters |
| (3.42.F) | $\gamma$ | Relativistic gamma factor (derived from the electron quantum motion |
| (5.6) | $T$ | CL space background temperature (by e⁻ param) |
| (5.12) | $T$ | CL space background temperature (by CL space parameters) |

*Note*: The calculated parameter *T* is for the Earth local field

| | | |
|--------|-----------|------|
| (5.13) | $E_{ZPE}$ | Zero Point Energy of single CL node |
| (5.14) | $E_{ZPE}(1m^3)$ | ZPE in 1 $m^3$ vacuum |
| (6.54) | | Hippoped curve in polar coordinates |
| (6.61) | $L_{pc}$ | Length of proton (neutron) core |
| (9.4) | E | Calculated energy potential for $H_2$ ortho-I, corresponding to experimental value of EVIP from PE spectrum |
| (9.17) | $C_{IG}$ | Product of IG constant and quadrature of intrinsic proton mass (Intrinsic product) |
| (9.55) | $\Delta E(p,n,\Delta)$ | Equation for vibrational levels for diatomic homonuclear molecules, where: A - is the atomic mass in atomic mass units (for one atom); p - is the number |

of protons involved in the bonding system (per one atom);

n - is a subharmonic quantum number of the quantum orbit; $r_n$ - is the internuclear distance at the equilibrium; $\Delta r$ - is a deviation from the equilibrium point; $\Delta$ - is a vibrational quantum number, referenced to equilibrium

| | | |
|--------|-----------|------|
| (9.26) | $\Delta r$ | Range of vibrational motion of protons in $H_2$ ortho-1 molecule |
| (10.11) | $E_{IFM}$ | Inertial force moment of folded CL nodes |
| (10.18) | $P_P/P_S$ | Ratio between Partial and Static CL pressure |
| (10.22) | $P_p$ | Specific partial pressure of CL space |
| (9.23) | $E_V$ | Energy levels of $H_2$ ortho-I molecule |
| (10.59) | $E_{IFM}^G$ | Inertial force moment in gravitational field |
| (12.50) | r | cosmological distance between distant galaxies where: z - redshift; $\tilde{L}$ - mean intergalactic distance; |
| (12.52) | $\tilde{n}$ | mean quasirefractive index of GSS; where: $(dN/dz)$ - is a line density measurable from Lyman alpha forests |

## 3. Used physical constants      Table 2

=============================================

| Constant | | Name |
|----------|---|------|
| $\alpha = 7.29735308\times10^{-3}$ | | fine structure constant |
| $c = 2.9979245\times10^{8}$ | (m/s) | light velocity |
| $\nu_c = 1.2355898\times10^{20}$ | (Hz) | Compton's frequency |
| $h = 6.6260755\times10^{-34}$ | (J.s) | Palnck's constant |
| $q = 1.60217733\times10^{-19}$ | (C) | elementary charge |
| $\mu_0 = 4\pi\times10^{7}$ | (N/A²) | permeability of free space |
| $\varepsilon_0 = 8.8541878\times10^{-12}$ | (C²/N m²) | permittivity of free space |
| $g_e = 2.0023193$ | | electron's gyromagnetic factor |
| $\mu_e = 9.2847701\times10^{-24}$ | (A m²) | electron's magnetic moment |
| $\mu_n = 9.6623707\times10^{-27}$ | (A m²) | neutron's magnetic moment |

Notes: (1) Additionally to the above constants, the rest masses of elementary particles as: proton, neutron, electron, pions,

muon, kaon are used. Two parameters from Electroweak theory also are used - the Fermi coupling constants, $G_F$ and the effective mixing parameter $\theta_{eff}^{lept}$. The measured mass equivalent energies of the bosons and tau are also used.

      (2) Large observational data material used by BSM is not presented in the abstract paper.

## 4. Calculated parameters        Table 3

==========================================
Parameter                 Name
--------------------------------------------------------------------

$R_c = 3.8615932\times10^{-13}$    (m)   Compton radius of electron

$s_e = 1.77061164\times10^{-14}$    (m)   helical step of the electron

$r_e = 8.842805\times10^{-15}$     (m)    small radius of the electron

$r_p = 5.895203\times10^{-15}$     (m)    small radius of the positron

$L_{pc} = 1.6277\times10^{-10}$   (m)    - proton's (neutron's) core length

$L_P = 0.667\times10^{-10}$    (m)     - proton's length

$W_P = 0.19253\times10^{-10}$   (m)     - proton's width

$2(R_c + r_p) = 7.841\times10^{-13}$   (m)   - proton's core thickness

$N_{RQ} = 0.88431155\times10^{9}$       number of resonance cycles contained in one SPM cycle

$\tau_{CL} = 0.0242631\times10^{-10}$   (s)   space-time constant of CL space

$k_d = 51.518$        ratio between the CL pumping time for 511 KeV photon and the space-time const

$k_{hb} = \sqrt{1 + 4\pi^2(0.6164^2)} = 4$   - derived from the concept of wavetrain width and Airy disk in diffraction limited optics (Eq. 1.20.a)

$d_{nb} = 1.0975\times10^{-20}$ (m)   $xyz$ node distance of CL space

$k_{rd} = 0.15$       equivalent trace radius of vibrating MQ type of node normalized to a node distance

$m_{CL} = 6.94991\times10^{-66}$   (kg)      inertial mass of the CL node estimated from Eq. (2.58)

$T = 2.6758$   (K)        CL space background temperature for the Earth local field

$C_{IG} = 5.2651\times10^{-33}$    (J m$^2$)

$E_{ZPE} = 4.43867\times10^{-48}$   (J/node)     - ZPE of single CL node

$E_{ZPE}(1m^3) = 3.35776\times10^{12}$   (J/m3)   - ZPE in 1 m$^3$ space

$P_S = 1.3735811\times10^{26}$   (N/m$^2$)      - Static CL pressure

$\rho_e = 1.52831\times10^{9}$   (kg/m$^3$)        - intrinsic electron density

$P_D = 2.0257865\times10^{3}$   (N/m$^2$Hz)    - Dynamical CL pressure

$E = 16.06$ (eV)        - theoretically derived system energy, corresponding to $E_{VIP} = 15.967$ eV from PE spectrum

$C_{IG} = 5.26511\times10^{-33}$    - intrinsic product

$\Delta r = 4\times10^{-16}$   (m)    - range of nuclear vibrational motion for $H_2$   ortho-I molecule (in absolute coordinate system)

$p_p = 3.343482\times10^{15}$   (N sec/m$^3$) - specific partial CL pressure

## 5. Abbreviations used in the abstract paper and the BSM thesis

BSM               Basic Structures of Matter (theory)
CL                 Cosmic Lattice
CL space       Cosmic Lattice space
EQ                 Electrical Quasisphere
FOHS          First Order Helical Structure
FQHE         Fractional Quantum Hall Effect
IG                 Intrinsic Gravitation
MQ               Magnetic Quasisphere
NRM           Node Resonance Momentum (vector)
RL                 Rectangular Lattice
RL(R)         Rectangular Lattice (Radial)
RL(T)         Rectangular Lattice (Twisted)
SPM           Spatial Precession Momentum (vector)
SOHS          Second order helical structure
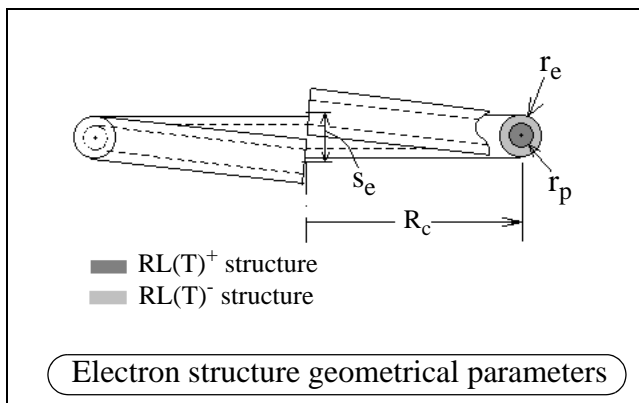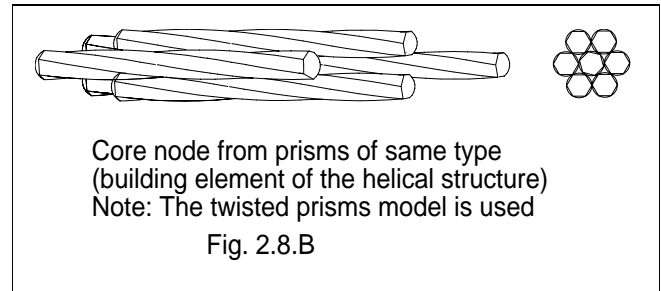ZPE           Zero Point Energy

## 6. References

[16] S. Sarg, "Basic Structures of Matter", thesis, (2001), http://www.helical-structures.org also in: http://collection.nlc-bnc.ca/amicus/index-e.html (AMICUS No. 27105955)

[17] S. Sarg, Atlas of Atomic Nuclear Structures (2001) http://www.helical-structures.org also in: http://collection.nlc-bnc.ca/amicus/index-e.html (AMICUS No. 27106037)

[18] S. Sarg, New approach for building of unified theory about the Universe and some results, http://lanl.arxiv.org/abs/physics/0205052 (2002)

Note: Full list of reference is included in the BSM thesis

## 6. Figures



Fig. 2.6

left handed   prism

right handed   prism

$d_{abcd}$

109.5   109.5 $^o$

109.5   109.5 $^o$

A - A

60 $^o$

60 $^o$



Core node from prisms of same type
(building element of the helical structure)
Note: The twisted prisms model is used

Fig. 2.8.B



$r_e$

$s_e$

$r_p$

$R_c$

RL(T)$^+$ structure
RL(T)$^-$ structure

Electron structure geometrical parameters



negative

central core   $e^-$   $e^-$ shell

$e^+$

$e^+$

$R_c$

Oscillating electron



protoneutron

$2(R_c + r_p)$

$\dfrac{L_{pc}}{\pi}$

$r_p$

$2R_c$

$L_{pc}$   proton

neutron

$W_p$

$L_p$

$L_{pc}/2\pi$

Shape and envelope structure of proton and neutron

Note: The parameters of the physical dimensions are given in Table 3.
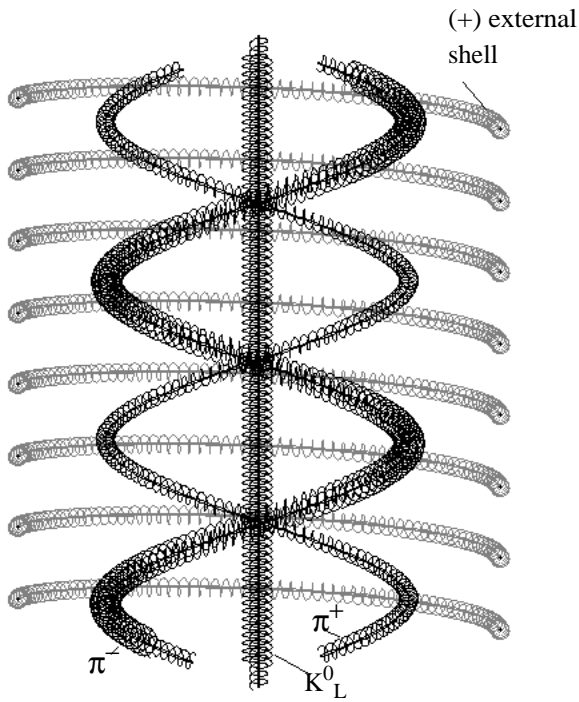
Fig. 2.15.B. Axial sectional view of proton (neutron) showing the external positive shell (envelope) and the internal subatomic particles. All of them are formed by helical structures with internal RL structures (not shown).



**b.**



**c.**

Fig. 2.16  Axial and radial section of FOHS showing the internal RL(R) type of structure (R - radial type).



Fig. 2.15.A. Radial sectional view of proton (neutron) core with internal subatomic particles and their internal RL structures. The RL structures are not twisted for the kaon, partly twisted for the pions and fully twisted for the external shell.
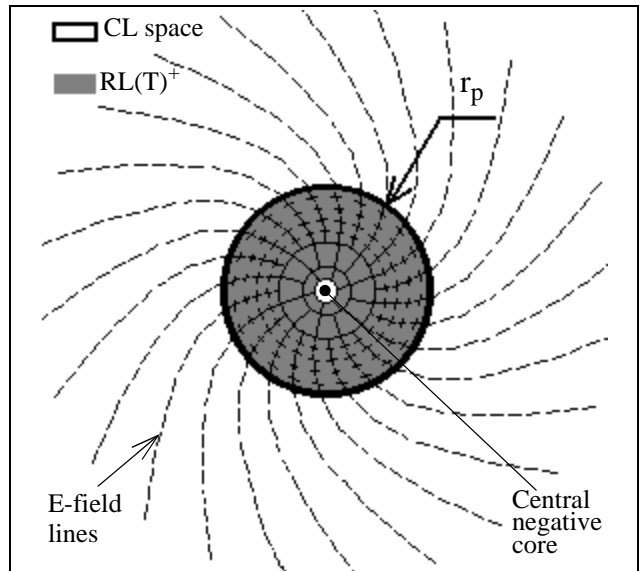


Fig. 2.29.E. Radial section of positive FOHS with twisted internal $RL(T)^+$ structure generating E-field in CL space. The radial section of the FOHS envelope core and the central core is formed of 7 prisms. $r_p$ - is a radius of the FOHS envelope.
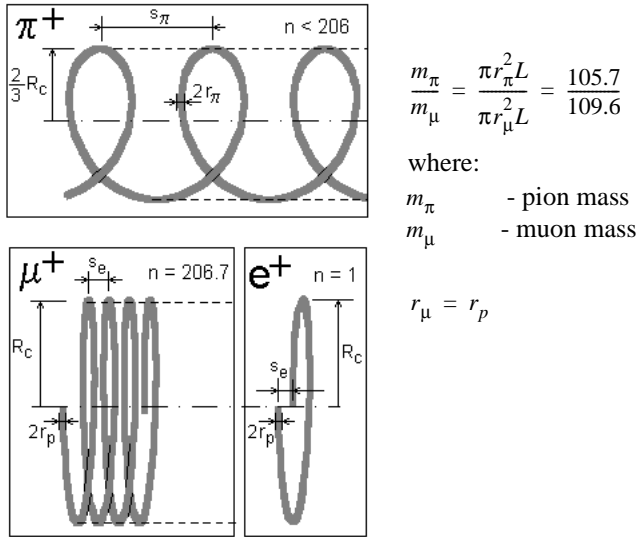
Fig. B. Pion - muon - positron decay. n - is number of helical turns, s - is the helical step, Rc is the compton radius. The "wired" length L of the helical structure in pion - muon conversion is unchanged, only the small radius is shrunk due to the internal RL twisting. Such twisting is possible after the internal pion with a curled torus shape is cut in one place (when the proton or neutron is cut due to a strong collision or impact). $r_\pi$, $r_\mu$, $r_p$ are respectively the small radii of the pion, muon and positron

$$\frac{m_\pi}{m_\mu} = \frac{\pi r_\pi^2 L}{\pi r_\mu^2 L} = \frac{105.7}{109.6}$$

where:

$m_\pi$    - pion mass

$m_\mu$    - muon mass

$$r_\mu = r_p$$



Deuteron with electron in Balmer series orbital



He nucleus (from Atlas of ANS)
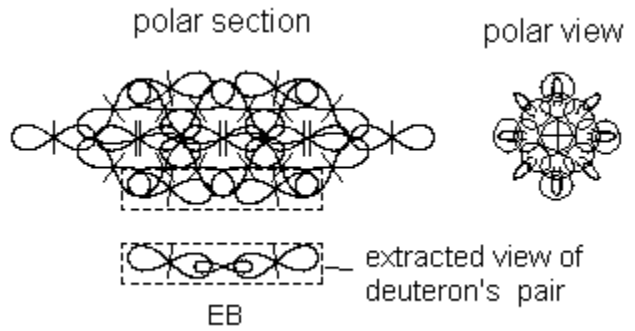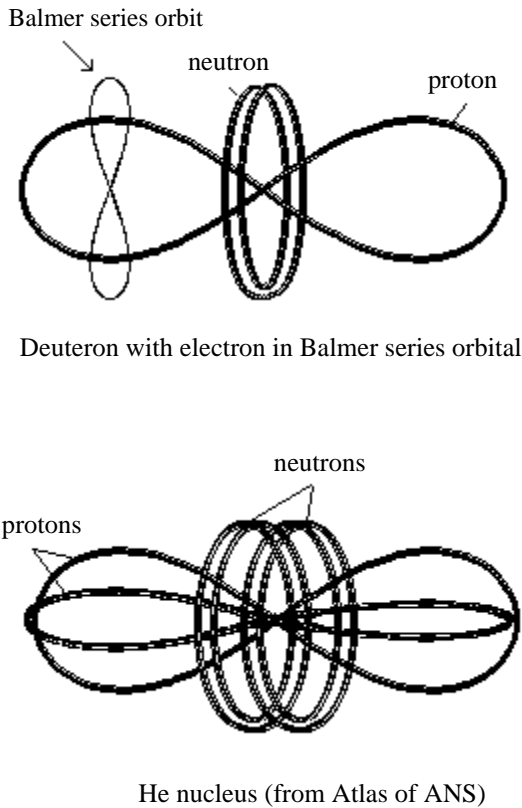


Fig. 8.6
Axial section and polar view of Gd nucleus. Two connected deuterons formed in Lantanides are shown in the bottom. The alpha particles from the heavy radioactive elements ori-i ginate from these type of formations.
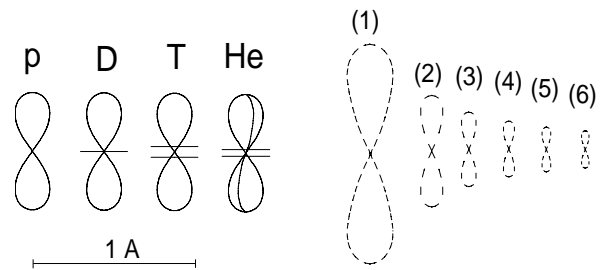


Fig. 9.3
Symbolic presentation of basic atomic structures (left) and quantum orbits with their subharmonic (velocity) number (right). The figure in brackets show the subharmonic number of the quantum orbit
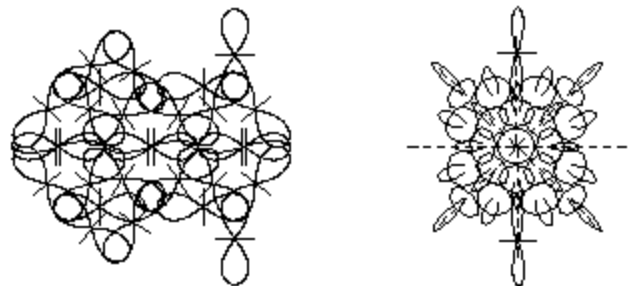


Axial section and polar view of Hg nucleus. The two valence electrons are in the external clubs of two deuterons (From Atlas of ANS)

(Physical model views for some other atomic nuclei are shown by ANS_selection.gif downloadable from the Atlas of ANS - reference source [2])

0 eV
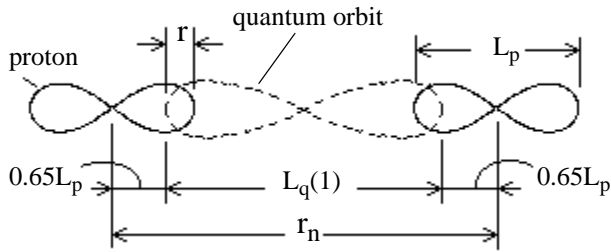
Fig. 9.12
Structure of $H_2$ - ortho-I state molecule

$L_p$ - is a proton length
$L_q(1)$ is a long side of first harmonic quantum orbit
$r_n$ - is the distance between the Hydrogen atoms
r - distance between the electron and the proton
core in the circular section (most external) of
the orbital trace

**Note:** The quantum orbit quasiplane does not coincide with the quasiplanes of the protons as shown in the Fig. 9.12 for drawing simplification. It is normal to the proton quasiplane and the orbit trace passes through the locuses of the protons Hippoped curves.

equilibrium internuclear distance (corresponding to the bottom of the vibrational curve).
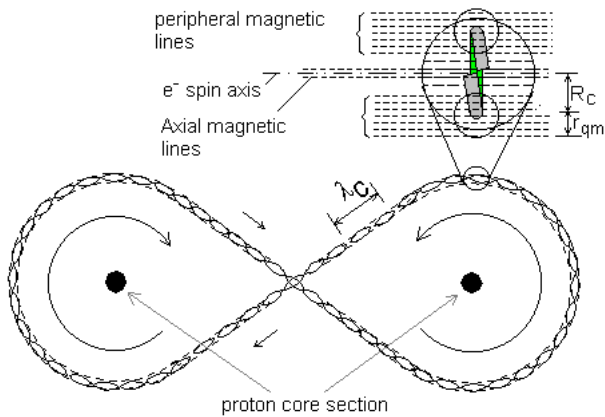


Fig. 7.7. Idealized shape of Balmer series orbit.
$R_c$ - is the Compton radius, $r_{qm}$ - is a magnetic radius of electron at suboptimal quantum velocity.
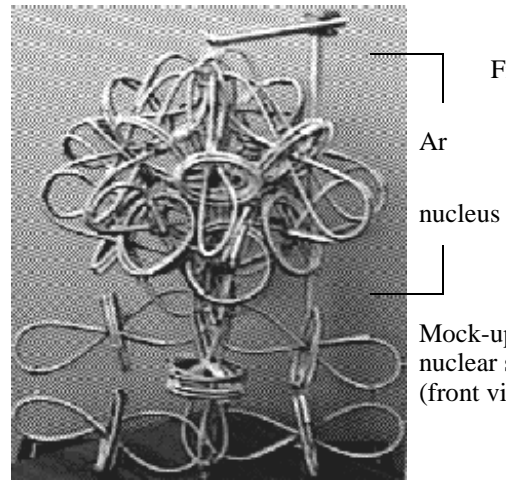


Fig. 8.23

Ar

nucleus

Mock-up of atomic nuclear structure (front view)
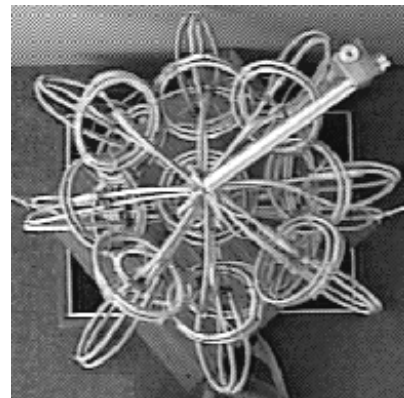


Fig. 8.24

Mock-up of atomic nuclear structure (polar view)
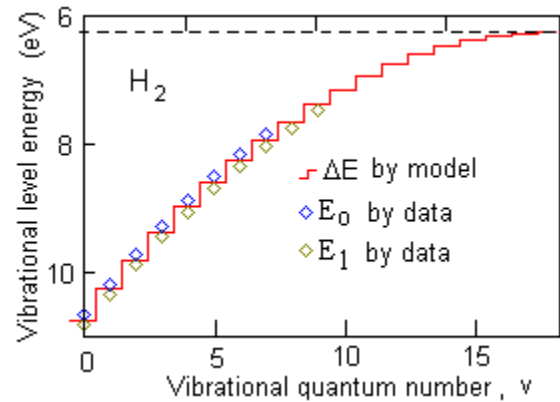


Fig. [9.24]. Energy levels $E_v$, (eV) calculated by Eq. (9.23) towards the vibrational levels for H2 - ortho. The calculated levels are shown by step line, while the optical transitions corresponding to two different QM spins are shown by diamonds.
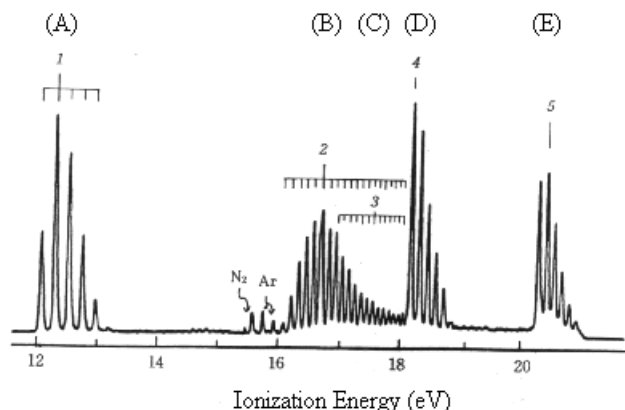
Fig. 9.42. PE spectrum of oxygen molecule excited by
He I radiation (Turner et all., courtesy of K. Kimura
et al., (1981))

Calculated by Eq. (9.55) values for $r_n$ for **Table 9.6**
$O_2$ states. The values are given in Angstroms (A).

| $r_n$ (A) | $L_q(2)$ (1 bond) | $L_q(2)$ (2 bonds) | $L_q(2x)$ (2 bonds) | $L_q(3)$ (2 bonds) |
|---|---|---|---|---|
| calculated | 2.57 A | 1.698 A | | 1.219 A |
| match drawing | 2 A | 1.7 A | 1.74 A | 1.25 A |
| possible state | {B}, {C} | {D} | {E} | {A} |

## 7. Examples of some molecular structures

Note: The nuclear particles in the central polar section of the
atomic nucleus are only shown.
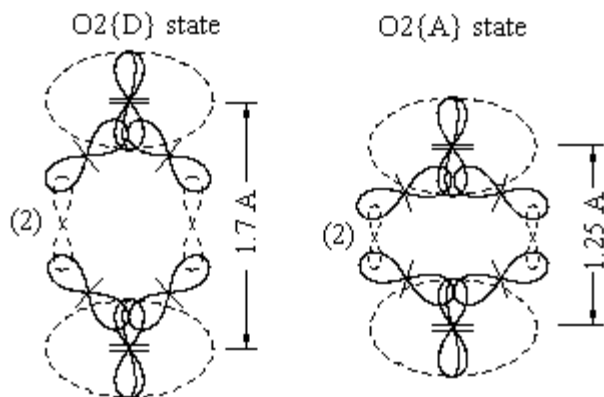


Fig. 9.43  Possible configurations of   $O_2(D)$ and $O_2(A)$.
{D} and {A} are states of $O_2$ according BSM model. The or-
bital planes of electrons does not lie in the drawing plane, but
are shown in this way for convenience. The number in brack-
et indicates the subharmonic number of the quantum orbit.
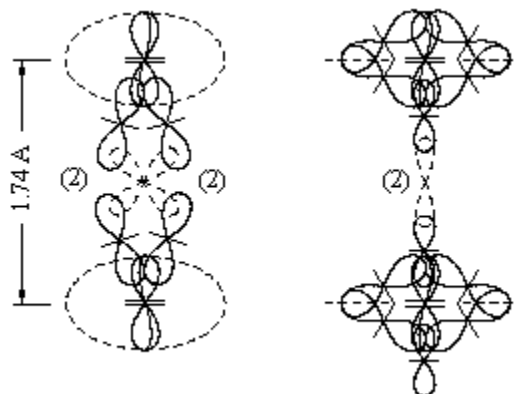


Fig.9.45
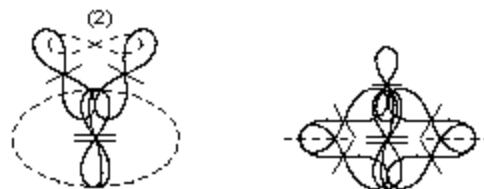Possible configuration of $O_2$ molecule in {E} state



Fig. 9.53
Two views of the possible configuration of oxygen
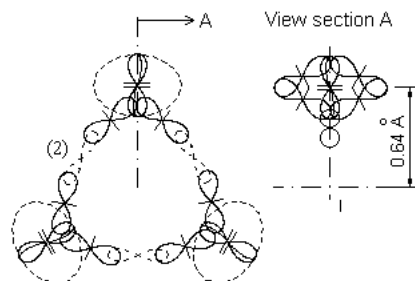atom in Airglow state responsible for line emissions
at 5577 A and 6300 A.



Fig. 9.53.A
Ozone molecule with second subharmonic bonding orbits
Every one of three bonding orbits contains two electrons
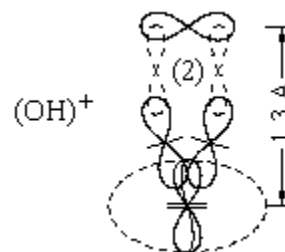with opposite quantum mechanical spin



Fig. 9.54. Possible configuration of $(OH)^+$
(the planes of  bonding orbits are shown rotated

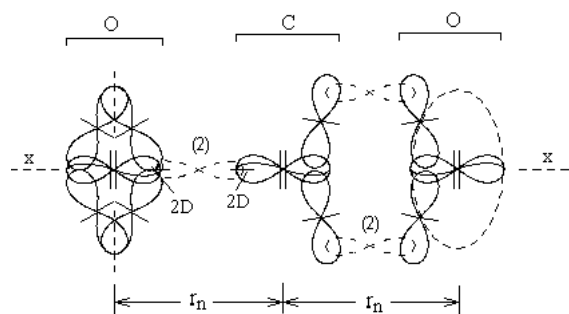at 90 deg, but in  the real physical model, they are normal to the drawing plane)



Fig. 9.56

One view of $CO_2$ molecule.  The oxygen atoms looks differently in both ends because the right-side one is rotated at 90 deg around  the $xx$ axis in respect to the left-side one.
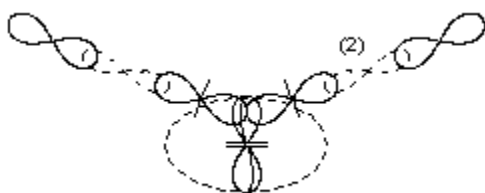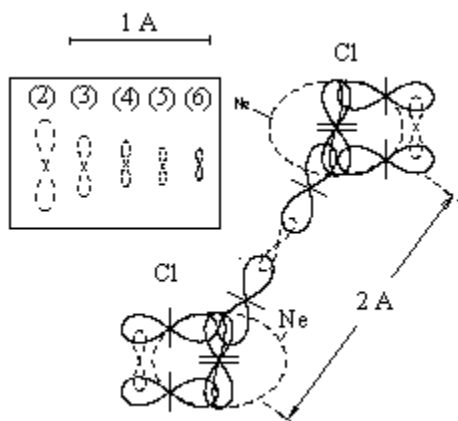


Fig. 9.59
Water molecule



Fig. 9.7 $Cl_2$ molecule. The dashed oval is the envelope of Ne nucleus. The set of possible quantum orbits are shown in the square box, the number in bracket is the subharmonic number of electron quantum velocity. The experimental value of internuclear distance between Cl atoms is 1.98 A.

**Notes:**
(1). The list of references used in the thesis are provided in the  full version of BSM.
(2) **About figures**: The numbered figures are from BSM thesis, others are from the Atlas of Atomic Nuclear Structures.